

See discussions, stats, and author profiles for this publication at: <https://www.researchgate.net/publication/322597773>

Lithium enrichment and isotopic variation in minerals from peridotite xenoliths from northwestern Ethiopian plateau

Article in *Journal of the Geological Society of India* - January 2018

DOI: 10.1007/s12594-018-0825-x

CITATIONS

0

READS

103

4 authors, including:



Melesse Alemayehu

Guangzhou Institute of Geochemistry, Chinese Academy of Science, Guangzhou, ...

23 PUBLICATIONS 20 CITATIONS

[SEE PROFILE](#)



Patrick Asamoah Sakyi

University of Ghana

86 PUBLICATIONS 1,318 CITATIONS

[SEE PROFILE](#)



Muhammed Haji

Chinese Academy of Sciences

6 PUBLICATIONS 12 CITATIONS

[SEE PROFILE](#)

Some of the authors of this publication are also working on these related projects:



Mantle Geochemistry: Influence of plume on continental lithosphere [View project](#)



Understanding the evolution of the Togo-Buém and Dahomeyan formations [View project](#)

Lithium Enrichment and Isotopic Variation in Minerals from Peridotite Xenoliths from Northwestern Ethiopian Plateau

Melesse Alemayehu^{1,2,*}, Hong-Fu Zhang^{1,3}, Patrick Asamoah Sakyi⁴ and Muhammed Haji⁵

¹ State Key Laboratory of Lithospheric Evolution, Institute of Geology and Geophysics, Chinese Academy of Sciences, P.O. Box 9825, Beijing 100029, China

² School of Applied Sciences, Department of Applied Geology, Adama Science and Technology University, P.O. Box 1888, Adam, Ethiopia

³ State Key Laboratory of Continental Dynamics, Department of Geology, Northwest University, Xi'an 710069, China

⁴ Department of Earth Science, University of Ghana, P.O. Box LG 58, Legon Accra, Ghana

⁵ Division of Engineering Geology and Water Resources, Institute of Geology and Geophysics, Chinese Academy of Sciences, P.O. Box 9825, Beijing 100029, China

*E-mail: melesse555@yahoo.com

ABSTRACT

We report Lithium (Li) concentrations and isotopic compositions for co-existing olivine, orthopyroxene (opx), and clinopyroxene (cpx) mineral separates from depleted and metasomatised peridotite xenoliths hosted by basaltic lavas from northwestern Ethiopian plateau (Gundeweyn area). The peridotites contain five lherzolites and one harzburgite and are variably depleted and enriched in LREE relative to HREE. In both depleted and enriched lherzolites, Li is preferentially incorporated into olivine (2.4-3.3 ppm) compared to opx (1.4-2.1 ppm) and cpx (1.4-2.0 ppm) whereas the Li contents of olivines (5.4 ppm) from an enriched harzburgite are higher than those of lherzolites. Olivines from the samples show higher Li abundances than normal mantle olivines (1.6-1.9 ppm) indicating the occurrence of Li enrichments through melt-peridotite interaction. The average $\delta^7\text{Li}$ values range from +2.2 to +6.0‰ in olivine, from -0.1 to +2.0‰ in opx and from -4.4 to -0.9‰ in cpx from the lherzolites. The Li isotopic composition (3.5‰) of olivines from harzburgite fall within the range of olivine from lherzolites but the opxs show low in $\delta^7\text{Li}$ (-2.0‰). Overall Li isotopic compositions of olivines from the peridotites fall within the range of normal mantle olivine, $\delta^7\text{Li}$ values of $+4\pm 2\%$ within uncertainty, reflecting metasomatism (enrichment) of the peridotites by isotopically heavy Li-rich asthenospheric melt. Li isotope zonation is also observed in most peridotite minerals. Majority of olivine grains display isotopically heavy cores and light rims and the reverse case is observed for some olivine grains. Orthopyroxene and clinopyroxene grains show irregular distribution in $\delta^7\text{Li}$. These features of Li isotopic compositions within and between grains in the samples reflect the effect of diffusion-driven isotopic fractionation during melt-peridotite interaction and cooling processes.

INTRODUCTION

The continental lithospheric mantle (CLM) beneath Ethiopian plateau and rift zone has experienced depletion and enrichment processes at different cales and periods (Roger et al., 1999; Conticelli et al., 1999; Ayalew et al., 2003; Reisberg et al., 2004). This is shown by the distinct compositions of mantle xenoliths found in the basaltic rocks of plateau and Cenozoic rift (Ferrando et al. 2008; Frezzotti et al. 2010; Meshesha et al. 2011; Beccaluva et al. 2011; Bianchini et al. 2014). Peridotites from the Ethiopian plateau particularly from the Gundeweyn area (Fig. 1) have 0.5-0.9 Ga Lu-Hf depletion and 0.4-0.6 Ga Sm-Nd enrichment ages (Alemayehu et al., 2016c). The Sm-Nd, Lu-Hf and Re-Os isotope systematic of the peridotites

indicate that the southern Ethiopian CLM formed between 0.9 to 2.8 Ga (Reisberg et al., 2004; Meshesha et al., 2011; Bianchini et al., 2014), providing strong indication that at least some parts of the lithospheric mantle beneath the southern Ethiopian rift zone were older than the plateau CLM. Many geophysical studies have showed low velocity anomalies related to the presence of anomalously hot and buoyant mantle upwelling beneath various parts of the East African rift including the Ethiopian plateau and rift zone (e.g. Ebinger et al., 1989; Nyblade et al., 2000; Debayle et al., 2001; Benoit et al., 2006). The low velocity anomalies are related to one or two mantle plumes (e.g. Ebinger and Sleep, 1998; George et al., 1998; Rogers et al., 2000) or of mantle upwelling (African super plume, Janney et al. 2002; Furman et al. 2004, 2006b) that triggered lithospheric thinning beneath East African rift (e.g. Ebinger and Casey 2001; Furman and Graham 1999; Rooney 2010). The geophysical investigation integrated with geochemical data of mantle xenoliths from Ethiopian Cenozoic basalts suggest that the present lithosphere is much hotter (60-150 mW/m²; Meshesha et al., 2011; Alemayehu et al., 2016a) than the actual continental lithospheric mantle (40 mW/m²; Pollack and Chapman 1977). Moreover, the investigated physicochemical changes leads to the formation of the Ethiopian CLM during the Pan-African time (e.g. Meshesha et al., 2011; Bianchini et al., 2014) followed by various types of metasomatic processes that have been related to eruption of plateau basaltic lavas connected to plume-related sub-alkaline magmatism (Beccaluva et al. 2011). Thus, the Ethiopian xenoliths provide special opportunity to address mantle process and evolution mechanism of modern lithospheric mantle, which is connected with the rising of the Afar plume. It is usually agreed that the Pan-African subduction and Cenozoic East African rifting are the two major geological events that affect the CLM beneath Ethiopian plateau and rift zone. The nature of the lithospheric mantle beneath Ethiopia also modified from the typical refractory to fertile (Alemayehu et al., 2016a). However, the processes related to peridotite-melt interaction are still not well constrained.

Many earlier worldwide studies have shown that most of the peridotites are affected by various degrees of peridotite-melt interaction (metasomatism), occurring at different lithospheric levels and causing significant geochemical modifications of the lithospheric mantle (e.g. Piccardo et al., 2007). Peridotite-melt interactions occurring in the Ethiopian CLM have been identified to be the result of multiple metasomatic overprints, that were initially associated with the Pan-African subduction and subsequently caused by small degree partial melts from the asthenospheric mantle or from mantle plume sources during the development of the East African rift system (EARS)

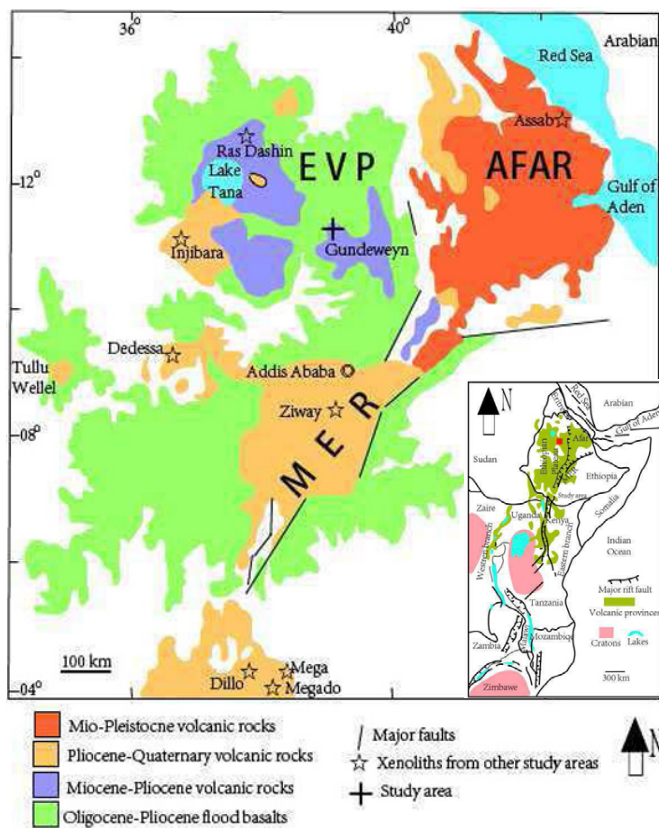


Fig.1. (a) The distribution of Neoproterozoic basement rocks and volcanic rocks in East Africa (Kamunzu and Mohr 1991) and the red square denote the location of the study area, **(b)** Distribution of Cenozoic volcanic rocks in Ethiopian plateau and rift zone (Ferrando et al. 2008). EVP and MER denote Ethiopian Volcanic Province and Main Ethiopian Rift, respectively. The location of the study area is shown by a cross (+).

(Rogers et al., 1999; Beccalva et al., 2011; Alemayehu et al., 2016b).

Li is a mobile element that preferentially enters the fluid phase during partial melting and fluid/melt-rock reaction processes in mantle (Brenan et al., 1998). The large mass difference between the two Li (${}^6\text{Li}$ ~7.59% and ${}^7\text{Li}$ ~92.41%) isotopes (~16%) cause significant Li isotopic fractionation during geological processes. The Li isotope system has been employed as a potential geochemical tool for tracing various melt/fluid-related geological processes for example continental weathering (Rudnick et al. 2004; Teng et al. 2010), seafloor alteration (Chan et al. 1992; Scholz et al. 2009), crust/mantle recycling (Tomascak et al. 2000; Brooker et al. 2004; Elliott et al. 2006) and peridotite-melt/fluid interactions (Rudnick and Ionov 2007; Zhang et al. 2010; Tang et al. 2011; Su et al. 2012).

In this work, new Li elemental and isotopic data on variably depleted and metasomatised mantle xenoliths entrained in alkaline basalt from northwestern Ethiopian plateau (Gundeweyn area) in order to further explain the characteristics of early and late stage geological processes occurring beneath the area are presented. These new results are integrated with the previous elemental and Sr isotopic studies (Alemayehu et al., 2016a) in order to further explore the compositional modification of CLM beneath Ethiopian plateau.

GEOLOGICAL SETTING AND ANALYSED SAMPLES

Geological setting

The Ethiopian volcanic province is covered dominantly by Tertiary and Quaternary basaltic rocks, ranging in thickness from 700 to 2000 m. It covers an area of several hundred kilometers across on the

plateau, on either side of the Main Ethiopian Rift (MER) and the Afar depression (Berhe et al. 1987; Fig. 1a). The MER, which is bounded by the Ethiopian plateau to the west and Somalian plateau to the east, extends northeast to southwest and widens at the Afar depression (e.g. Baker et al., 1972; Fig. 1). Volcanism of the Ethiopian plateau is mainly confined to major deep-seated fractures, which were reactivated during rifting of the EARS. Most eruptions were contemporaneous with the collision of the Arabian and Eurasian plates (Hampton 1987), and took place in northwest to southeast trend.

The thick sequence of late Eocene to early Miocene flood basalts of Ethiopian plateau is overlain by less voluminous late Miocene to Quaternary lavas erupted from several distinct shield volcanoes; their ages vary from <29 to 3 Ma (Kieffer et al., 2004). The shield volcanoes consist of alternating basaltic and rhyolitic lava flows, tuffs and ignimbrites. Kieffer et al. (2004) found both tholeiitic and alkaline volcanic rocks from shield volcanoes from northwestern Ethiopian plateau with ages comparable with the flood basalts. They described the large variation in the incompatible element contents of the two volcanic series in terms of differences of source composition and degree of partial melting, and concluded that the lavas from the plateau were formed from a broad region of upwelling mantle, that was thermally and compositionally heterogeneous. Conversely, Tommasini et al. (2005) suggested that plateau mafic lavas are derived from a fertile and vertically zoned enriched CLM with relatively homogeneous lateral continuity at a pressure of about 23.5 GPa. Finally, Furman et al. (2006) reported that the geochemical difference between the Oligocene-Quaternary continental flood basalts of the plateau and the Quaternary rift basalts are probably not related to significant changes in lithospheric source composition but to depth and degree of melting as well as mixing processes involving depleted, moderately enriched and metasomatised mantle domains.

The Gundeweyn volcanic field is located in east Gojam, northwestern Ethiopian plateau and contains mantle xenoliths in the late Miocene alkali basalts dated at 23.1 Ma (Kieffer et al., 2004). The volcanic field is mainly composed of lava flows, trachyte plugs and scoria cones. The pyroclastic and volcanic rocks contain dominantly scoria and olivine-phyric basalts. The basaltic lavas and monogenetic scoria cones enclose various types of fresh mantle xenoliths as described below.

Analysed Samples

Six (five lherzolites and one harzburgite) peridotite xenoliths collected from the Gundeweyn volcanic field were studied in this work. The samples are very fresh and, show protogranular and porphyroclastic textures. The primary mineral assemblages are olivine, orthopyroxene, clinopyroxene and spinel with minor amphiboles (Table 1). The minerals vary in size from 1 to 5 mm with subhedral to anhedral profile. A few orthopyroxene contains lamellae of clinopyroxene and vice versa. The olivines have Fo content, which is equivalent to Mg# ($= 100 \times \text{Mg}/(\text{Mg} + \text{Fe})$), in the range from 89.3 to 89.8 with higher values from the harzburgite (Table 1). Based on CI-normalized REE patterns, the clinopyroxene from lherzolites can be classified into two groups (Fig. 2): depleted (GT272, GT278 and GT2716) which are characterized by a distinct depletion in LREE and enriched (GT273 and GT275) which are characterized by enrichment in LREE relative to MREE and HREE. The clinopyroxene from harzburgite (GT2713) is categorized into enriched group with lower MREE-HREE abundances than the lherzolites. Clinopyroxenes from lherzolite have ${}^{87}\text{Sr}/{}^{86}\text{Sr}$ of 0.70227 to 0.70357, ${}^{143}\text{Nd}/{}^{144}\text{Nd}$ of 0.51285 to 0.51346, and ${}^{176}\text{Hf}/{}^{177}\text{Hf}$ of 0.28297 to 0.28360. These values range between depleted mantle and the HIMU mantle end-member. Overall, the petrography combined with detailed major-trace element and Sr-Nd-Hf isotope characteristics of the Gundeweyn peridotites reflect

Table 1. GPS location, modal abundances (vol.%), selected elemental composition and textures of Gundweyn (GT) mantle xenoliths

Sample	GPS location (degree)		Modal mineralogy (Vol. %)					Fo			Texture	Rock type
	Easting	Northing	olivine	opx	cpx	spl	amph	olivine	(La/Yb) _N	(Dy/Lu) _N		
GT272	38.156	10.963	56	23	18	2		89.6	0.45	0.95	Protogranular	Depleted lherzolite
GT273	38.158	10.964	51	28	19	2	trace	89.5	2.92	1.52	Protogranular	Enriched lherzolite
GT275	38.159	10.964	60	24	15	1	trace	89.3	3.06	1.40	Protogranular	Enriched lherzolite
GT278	38.161	10.965	51	28	19	2		89.6	0.24	1.06	Porphyroclastic	Depleted lherzolite
GT2713	38.161	10.951	69	27	3	1	trace	89.8	34.5	0.86	Porphyroclastic	Enriched harzburgite
GT2716	38.163	10.946	70	19	10	1	trace	89.6	0.25	1.18	Porphyroclastic	Depleted lherzolite

Fo = forsterite content; Mg# = molar 100Mg/(Mg+Fe), nomenclature after Mercier and Nicolas (1975)

N = normalized to chondrite after Sun and McDonough (1989)

the occurrence of variable degree of partial melting and metasomatic overprint at different times (Alemayehu et al. 2016a,c).

ANALYTICAL METHODS

Mineral separations and, Li elemental and isotope analysis were carried out at the State Key Laboratory of Lithospheric Evolution, Institute of Geology and Geophysics, Chinese Academy of Sciences, China. Olivine, orthopyroxene and clinopyroxene separates were handpicked under binocular stereomicroscope. In situ Li concentration and isotope analyses of olivines and pyroxenes on gold coated grain mounts were performed using a Cameca IMS-1280 ion microprobe following the techniques of Zhang et al. (2010) and Su et al. (2012, 2015). A 13 kV, 10-20 nA oxygen primary beam was focused on spot size of 20 μm in diameter. A 60 s pre-sputtering was applied without raster before analysis. A 10 kV was used to accelerate a positive secondary ion, which is measured at medium mass resolution ($M^{3\%}M \sim 1100$) with 125mm aperture without energy offset. The primary beam position, entrance slits, contrast aperture, magnetic field and energy offset were automatically centered prior to each measurement. Secondary ions were counted on mono-collection pulse counting mode. 30 to 40 cycles were measured with counting time of 12 s for ^6Li , 4 s for ^7Li and 4 s for background at 6.5 mass. The counting rate on ^7Li range from 30,000 to 100,000 cps based on the Li content of the sample and the primary beam intensity. Li isotopic ratios are given in delta units using the $\delta^7\text{Li}$ notation ($\delta^7\text{Li} = [({}^7\text{Li}/{}^6\text{Li}_{\text{sample}}) / ({}^7\text{Li}/{}^6\text{Li}_{\text{L-SVEC}}) - 1] * 1,000$ relative to the L-SVEC Li isotope standard, with ${}^7\text{Li}/{}^6\text{Li}_{\text{L-SVEC}} = 12.0192$, Flesch et al., 1973)). 06JY31ol for olivine, 06JY31opx for orthopyroxene and 06JY31cpx for clinopyroxene (Su et al. 2015) were used as standards and gave the average values of $\delta^7\text{Li} = 4.75 \pm 0.8\%$, $-0.24 \pm 0.9\%$ and $-2.47 \pm 1.0\%$, respectively, which

fall in the range of previously published values within analytical uncertainty ($\delta^7\text{Li} = 4.51\%$, -0.19% and -2.37% , respectively; Su et al., 2015).

RESULTS

Olivine, orthopyroxene and clinopyroxene Li abundances and isotope compositions of the peridotite are given in Table 2. Clinopyroxene from the lherzolites show negative Li anomaly relative to the neighboring trace elements (Fig. 2). Because limited amount of clinopyroxene, Li content and isotopic compositions were not measured from harzburgites. A limited range in Li abundances and large variation in $\delta^7\text{Li}$ values are observed either within or among mineral grains in a sample (Fig. 3a, b). LREE-depleted and enriched samples do not show clear systematic differences in both Li abundances and $\delta^7\text{Li}$ (Fig. 3c, d).

In lherzolite, olivine exhibit variable Li abundances and $\delta^7\text{Li}$ values, ranging from 2.4-3.5 ppm and 1.8 to 6.3‰ for depleted and, 2.3-2.4 ppm and 2.4 to 4.2‰ for enriched samples (Fig. 4a). With the exception of some grains from GT275 and GT278, some olivines from depleted and enriched samples have higher $\delta^7\text{Li}$ in the cores than in the rims. Olivines from both depleted and enriched sample show higher Li contents relative to mantle olivines (1.6-1.9 ppm; Eggins et al. 1998; Seitz and Woodland, 2000). Olivines reveal negative correlations between Fo content and $\delta^7\text{Li}$ (Fig. 4b). The range of Li contents and isotopic compositions in orthopyroxene of lherzolites range from 1.4-2.2 ppm and -1.1 to 1.3‰ for depleted with exception for one core grain of 6.8‰, and 1.3-2.1 ppm and 0.7 to 1.3‰ for enriched samples (Fig. 4c). Some orthopyroxenes from depleted and enriched samples have lower $\delta^7\text{Li}$ in the cores than in the rims and some of the grains show irregular distribution in $\delta^7\text{Li}$, GT273 and GT278 samples. The Li abundance and $\delta^7\text{Li}$ obtained in clinopyroxene from depleted lherzolite (1.4-2.0 ppm; -5.6 to -0.5‰) is relatively wider compare to enriched once (1.3-1.4 ppm; 1.5 to -3.6‰) (Fig. 4d). Similar to orthopyroxenes, some clinopyroxenes from depleted and enriched samples have lower $\delta^7\text{Li}$ in the cores than in the rims and some grains show the opposite trend (GT2716). In a harzburgite (GT2713), olivines show homogeneous composition and higher Li abundances (5.4-5.5 ppm) than olivines from lherzolite. The $\delta^7\text{Li}$ values of olivines vary from 3.2 to 3.8‰ and increase from the core to the rim (Fig. 3b). Orthopyroxenes are also homogeneous in Li contents (1.3-1.4 ppm) and variable in $\delta^7\text{Li}$ (-4.3 to -0.4‰) with irregular rim-core-rim zonation.

In general, olivines Li concentration from each depleted and enriched peridotites are usually homogeneous and higher than those of coexisting pyroxenes (Fig. 3c). The clinopyroxenes show more or less similar Li contents with coexisting orthopyroxenes (Fig. 3c). Moreover, olivines $\delta^7\text{Li}$ are mostly higher than those of coexisting pyroxenes with clinopyroxene having lower $\delta^7\text{Li}$ than coexisting orthopyroxenes (Fig. 3d). With some exceptions, most olivines grains show higher Li isotopic compositions in the core than in the rims and the reverse case is observed for some olivine grains. Similarly, some

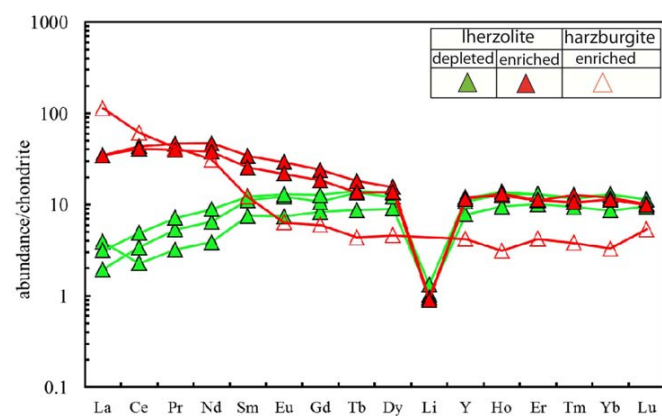


Fig. 2. Chondrite (CI) normalized REE and Li variation diagrams of clinopyroxene from Gundweyn mantle xenoliths. The data for REEs are from Alemayehu et al. (2016a) and the Li data is average analysis from this study. Normalizing values are from Sun and McDonough (1989).

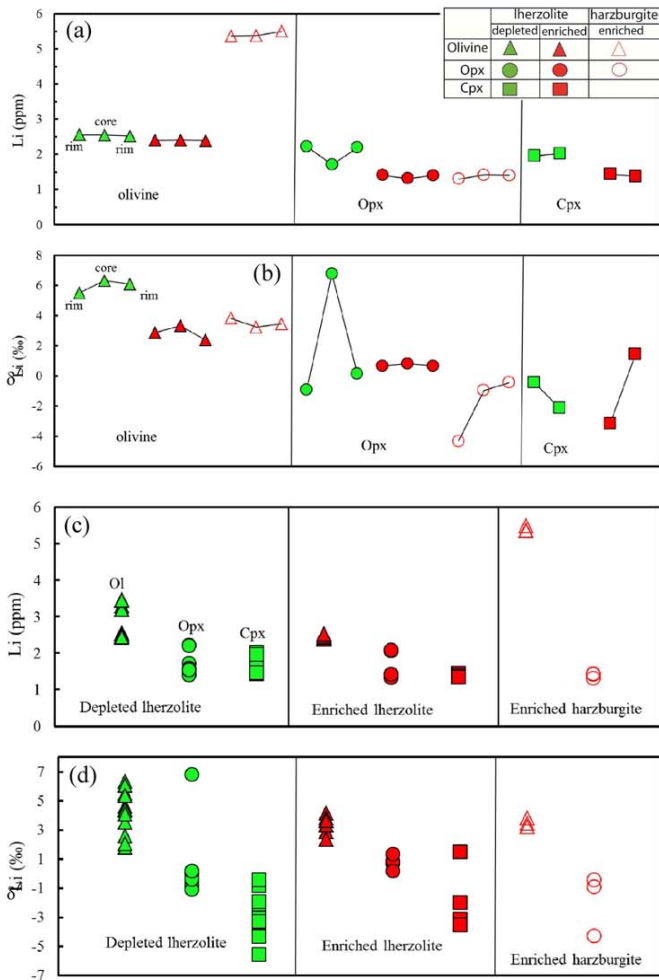


Fig.3. Li abundances (a) and isotopic compositions (b) of olivine, orthopyroxene and clinopyroxene core-rim. Comparison of Li abundances (c) and isotopic compositions (d) between depleted and enriched olivine, orthopyroxene and clinopyroxene minerals of Gundeweyn (GT) lherzolites and harzburgite. Triangle, circle and square represent olivine, Opx and Cpx, respectively.

orthopyroxene and clinopyroxene minerals show heavy rims and light cores and in some other grains it is opposite. Among the samples, olivines from the harzburgite and lherzolite show the highest Li abundances and $\delta^7\text{Li}$, respectively. Compared to most olivines reported from worldwide peridotites, olivines from Gundeweyn harzburgite show higher Li contents (Fig.4a).

DISCUSSION

Li Elemental Enrichment in Peridotite Xenoliths

Two groups of peridotite xenoliths can be identified from clinopyroxene REE patterns (Alemayehu et al. 2016a; Fig.2): depleted groups (lherzolites) show low contents of LREE and enriched groups (lherzolite and harzburgite) have relatively high contents of LREE relative to medium and heavy REE. These features are similar to those reported in the most of mantle peridotites worldwide and are generally explained as a result of different degrees of partial melting followed by metasomatic enrichments in incompatible elements (e.g. McDonough and Frey, 1989; Pearson et al. 2003). In general, the contents of compatible and moderately incompatible elements in peridotite series are mainly related to indices of melt extraction whereas those of highly incompatible elements are controlled by style and degree of metasomatic overprint. Li is a mobile and moderately incompatible

element that favorably enters to the fluid phase during partial melting and fluid/melt-rock reaction in mantle processes (Brenan et al. 1998). Generally, melt depletion related to partial melting leads to decrease in Li contents in mantle minerals due to the moderate incompatibility of Li whereas melt addition leads to increase in Li contents (e.g. Seitz and Woodland 2000). Most peridotite xenoliths show constant variation of Li content (olivine < orthopyroxene < clinopyroxene) among mantle minerals. This is because of Li diffusion rate in olivine is much slower than in pyroxene under similar environments (Parkinson et al. 2007; Dohmen et al. 2010; Coogan, 2011; Yakob et al. 2012), and on the other hand the partitioning of Li changes with cooling as it diffuses from olivine into clinopyroxene with lowering of temperature (Ionov and Seitz, 2008). In contrast, different trends in the variation of Li abundances in mantle peridotites, particularly the reverse sequence in Gundeweyn peridotite of this study have been observed (Fig. 3c and Table 2), which is in similar order of those found in equilibrated mantle peridotites (Ottolini et al. 2004; Seitz and Woodland, 2000). These Li compositional distributions between olivine, orthopyroxene and clinopyroxene are possibly related to early fractional crystallization and consistent with the report of Su et al. (2014). Olivine is the most abundant mantle mineral thus most of the Li budget in mantle peridotite is controlled by olivine, and commonly has Li abundances (1.6–1.9 ppm) which are a little higher than those of coexisting pyroxenes (Ryan and Langmuir 1987; Brenan et al. 1998; Eggins et al. 1998; Seitz and Woodland 2000). The distinct negative Li anomaly relative to other trace elements in clinopyroxenes from depleted and enriched Gundeweyn lherzolites (Fig. 2) indicates that Li in these mantle samples is preferentially incorporated into olivine. Olivines from peridotite samples in this study show higher Li concentrations than mantle olivine indicates that Li addition took place during and/or short time after fractional crystallization (Table 2). In Fig. 5a, all the peridotites samples fall away from the melt depletion field indicating that the peridotites are affected by the metasomatic melt. Olivine from depleted (2.4-3.5) and enriched (2.3-2.4 ppm) lherzolites show narrow range in Li

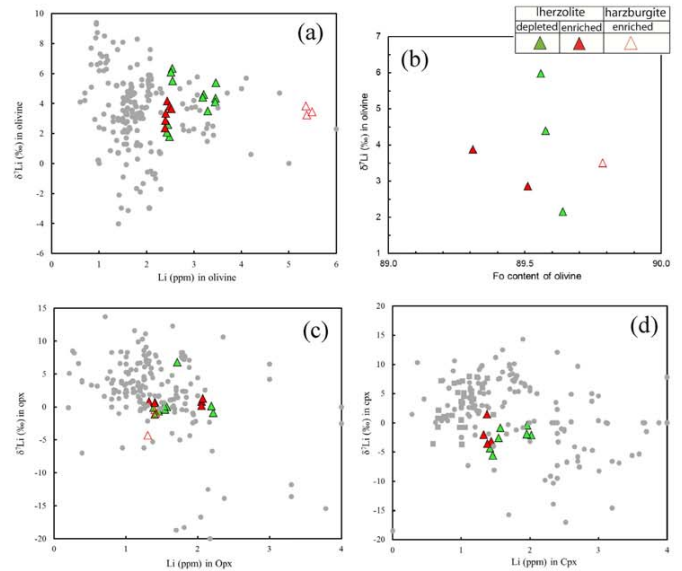


Fig.4. (a) Variation of Li abundances with $\delta^7\text{Li}$ of olivine, (b) average $\delta^7\text{Li}$ against Forsterite (Fo) content of olivine. Variation of Li abundances with $\delta^7\text{Li}$ of (c) orthopyroxene and (d) clinopyroxene, compared to worldwide xenoliths data (gray symbols). Data sources for worldwide xenoliths: Nishio et al. (2004), Seitz et al. (2004), Magna et al. (2006), Jeffcoate et al. (2007), Rudnick and Ionov (2007), Halama et al. (2009), Tang et al. (2007, 2011), Wagner and Deloule (2007), Ionov and Seitz (2008), Aulbach and Rudnick (2009), Zhang et al. (2010).

Table 2. *In-situ* Li abundance and isotopic compositions of olivine, orthopyroxene and clinopyroxene from Gundeweyn (GT) mantle xenoliths

Sample	Position	Olivine		Sample	Position	Orthopyroxene		Sample	Position	Clinopyroxene	
		Li (ppm)	$\delta^7\text{Li}$ (‰)			Li (ppm)	$\delta^7\text{Li}$ (‰)			Li (ppm)	$\delta^7\text{Li}$ (‰)
GT2720l@1	rim	2.55	0.05	5.51	0.85	GT2720px@1	rim	2.21	0.04	-0.91	0.94
GT2720l@2	core	2.55	0.04	6.34	0.90	GT2720px@2	core	1.72	0.02	6.78	1.07
GT2720l@3	rim	2.52	0.04	6.09	0.86	GT2720px@3	rim	2.19	0.04	0.14	0.94
GT2730l@1	rim	2.40	0.04	2.87	0.93	GT2730px@1	rim	1.41	0.03	0.66	1.18
GT2730l@2	core	2.41	0.04	3.33	0.89	GT2730px@2	core	1.32	0.03	0.83	1.21
GT2730l@3	rim	2.39	0.04	2.37	0.88	GT2730px@3	rim	1.40	0.03	0.66	1.18
GT2750l@1	rim	2.44	0.04	4.17	1.00	GT2750px@1	rim	2.05	0.04	0.84	1.03
GT2750l@2	core	2.49	0.04	3.82	0.89	GT2750px@2	core	2.07	0.04	0.17	0.97
GT2750l@3	rim	2.52	0.04	3.64	1.05	GT2750px@3	rim	2.07	0.04	1.30	0.97
GT2780l@1	rim	3.29	0.06	3.51	0.76	GT2780px@1	rim	1.39	0.03	-0.08	1.18
GT2780l@2	core	3.21	0.06	4.60	0.86	GT2780px@2	core	1.46	0.03	-0.68	1.15
GT2780l@3	rim	3.19	0.05	4.42	0.77	GT2780px@3	rim	1.40	0.03	-1.11	1.17
GT2780l2@1	rim	3.46	0.06	5.38	0.75	GT2713Opx@1	rim	1.30	0.02	-4.33	1.22
GT2780l2@2	core	3.45	0.06	4.36	0.75	GT2713Opx@2	core	1.42	0.03	-0.95	1.17
GT2780l2@3	rim	3.45	0.06	4.09	0.73	GT2713Opx@3	rim	1.40	0.03	-0.44	1.17
GT27130l@1	rim	5.36	0.09	3.83	0.72	GT2716Opx@1	rim	1.57	0.03	0.02	1.11
GT27130l@2	core	5.38	0.09	3.24	0.76	GT2716Opx@2	core	1.54	0.03	-0.40	1.11
GT27130l@3	rim	5.50	0.10	3.45	0.81	GT2716Opx@3	rim	1.53	0.03	0.16	1.12
GT27160l@1	rim	2.48	0.04	1.79	0.94						
GT27160l@2	core	2.45	0.04	2.59	0.86						
GT27160l@3	rim	2.43	0.04	2.07	1.04						

abundances. Most of the peridotites show generally homogenous Li abundances (Table 2) indicating the occurrence of Li enrichment for longer time to homogenize the Li within the grains. The concentrations of Li in olivines do not correlate well with the modal abundance of olivine (Fig. 5a) and with the degree of LREE enrichment of the peridotites, as measured by the chondrite-normalized $(\text{La}/\text{Yb})_N$ ratio of clinopyroxene (Fig. 5b). These features suggest that Li addition and LREE enrichment occur at different times within lithospheric mantle beneath Gundeweyn. Moreover, the Li enrichments do not appear to be correlated with the presence of metasomatic accessory minerals for example amphibole (Table 1). Interestingly olivines from the enriched harzburgites show Li enrichments (average 5.4 ppm) than those from lherzolites. This characteristic could be related to preferential enrichment of incompatible trace elements including Li in olivine-rich matrices relative to pyroxene (Toramaru et al. 1986; von Bagen et al. 1986; Van Orman et al. 2001; Rudnick et al. 2007). Another interesting feature is that Li abundance in olivines from harzburgite is higher than most olivines from worldwide peridotites (Fig. 4a). These observations suggest that the lithospheric mantle beneath the Gundeweyn region is influenced by large melt derived from the asthenospheric mantle, probably connected with the rising of the Afar plume which is near northeast of Gundeweyn. Like olivine,

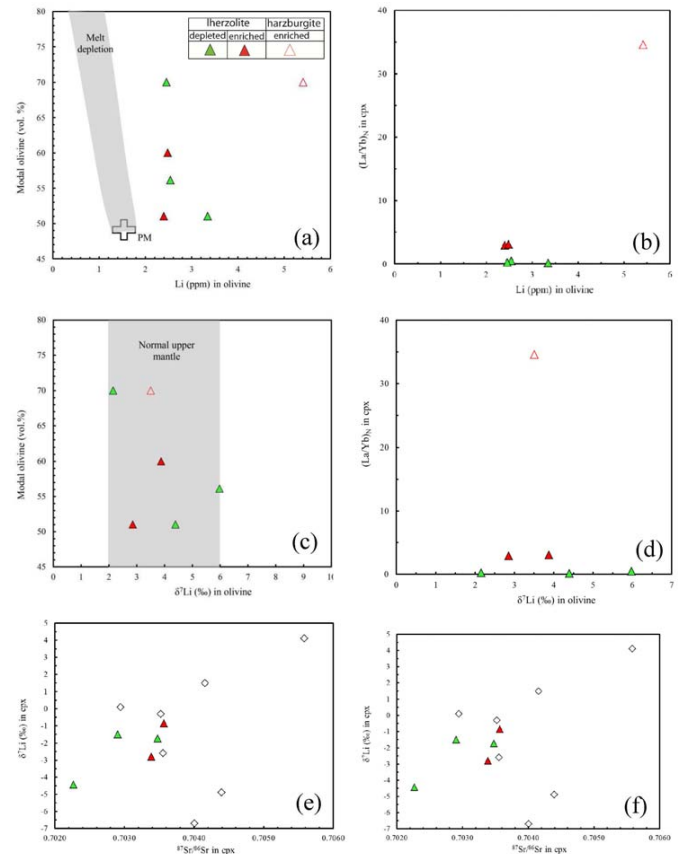


Fig.5. Lithium abundances (ppm) in olivine versus (a) modal olivine (vol. %) and (b) $(\text{La}/\text{Yb})_N$ in clinopyroxene. The gray field melt depletion is from Eggin et al. (1998); Seitz and Woodland (2000) and PM denotes primitive mantle from McDonough and Sun (1995). Lithium isotopic compositions (‰) in olivine versus (c) modal olivine (vol.%) and (d) $(\text{La}/\text{Yb})_N$ in clinopyroxene. The vertical gray field represents range of $\delta^7\text{Li}$ for normal upper mantle (Tomascak 2004). (e) $^{87}\text{Sr}/^{86}\text{Sr}$ against $\delta^7\text{Li}$ (‰) in clinopyroxene (f) Oxygen isotope compositions (‰) against $\delta^7\text{Li}$ (‰) in olivine. Data for Sr and O isotopic compositions are from Alemayehu et al. (2016a, d). Diamond symbols represent data for Tanzanian peridotite (Aulbach et al. 2008; Aulbach and Rudnick 2009) for comparison.

orthopyroxene and clinopyroxene show limited range in Li contents (Fig. 4c, d; Table 2). It is understood that olivine crystallizes before pyroxenes at mantle depth and temperature. The higher Li abundance in olivine than pyroxenes (Fig. 3c) indicates that Li is incorporated into mineral in the early stage of melt/magma fractionation at mantle temperature. This is consistent with the earlier experimental and empirical results that Li is moderately compatible element for olivine (Chan et al., 1992; Dohmen et al., 2010; Caciagli et al., 2011).

Variation of Li Isotope Compositions in Mantle Peridotite

Diffusion is an essential mechanism for Li isotopic variation in mantle peridotites. The diffusion rate of ^6Li about 2–3% faster than ^7Li (Richter et al. 2003; Coogan et al. 2005; Lundstrom et al. 2005) regardless of other physical factors like temperature and pressure as well as melt composition. On the other hand, the Li diffusion rate is highly variable in different mantle minerals which might be linked to temperature (Wunder et al., 2006; Ionov and Seitz 2008; Dohmen et al., 2010; Caciagli et al., 2011; Coogan, 2011; Yakob et al., 2012). Accordingly, the isotopic fractionation of Li will be accompanied by the preferential incorporation of Li into minerals. Ionov and Seitz (2008) reported that the abnormal and disequilibrated isotopic compositions of Li in peridotite xenoliths might be linked to the redistribution of Li between minerals, but they attributed it to the post-eruptive cooling process. Minerals from our samples show systematic $\delta^7\text{Li}$ variation (Fig. 3d; Table 2) with olivine (1.8 to 6.3‰) > orthopyroxene (-1.1 to 1.3‰) > clinopyroxene (-5.6‰ to 1.5‰). The overall decreasing $\delta^7\text{Li}$ value from olivine to both orthopyroxene and clinopyroxene implies that fractional crystallization can result in Li isotopic fractionation of the melts/magmas followed by melt additions into the peridotites. The Li rich and high $\delta^7\text{Li}$ character of olivines in Fe-rich peridotites and the deep-seated garnet-bearing peridotites from Tanzanian are described to be related to a prolonged melt-peridotite interaction event linking to plume related silicate melts connected with the East Africa rift (Aulbach et al. 2008). This is consistent with present observations. It is expected that Gundeweyn peridotites, including olivine, have experienced metasomatic overprinting during earlier phases of East Africa rift magmatism, which may be related to Pan-African subduction (Alemayehu et al. 2016a). The Li isotopic compositions of olivines from Gundeweyn peridotites fall within the range of normal mantle olivine, $\delta^7\text{Li}$ values of $\sim +4 \pm 2\%$ within uncertainty (Fig. 5c), reflecting metasomatism (enrichment) of the peridotites by isotopically heavy Li-rich asthenospheric melt. Moreover, the rough negative correlations between $\delta^7\text{Li}$ and forsterite content in olivine (Fig. 4b) suggest that the peridotites are the results of interaction between lithospheric mantle and isotopically heavy Li rich melt. Comparable interaction between $\delta^7\text{Li}$ depleted lithospheric mantle with a Li rich and isotopically heavy melt has been suggested for south Africa cratonic peridotites (Bell et al., 2005), but it is unclear whether the relatively light Li in ancient refractory mantle is due to earlier melt addition or whether it reflects a secular evolution toward more isotopically heavy mantle due to addition of high $\delta^7\text{Li}$ crustal components (Bell et al. 2005). However, Aulbach et al. (2008) infer that the Tanzania peridotites are the results of interaction between isotopically light ancient lithospheric mantle and isotopically heavy Li rich melt. Similar interpretation can be applied for Gundeweyn peridotites that the lithospheric mantle beneath northwestern Ethiopia experienced isotopically heavy Li rich melt-peridotite reactions.

Majority of olivine grains from Gundeweyn peridotite display isotopically heavy cores and light rims and few of the olivine grains show the reverse relation. These indicate that initially the peridotite is metasomatized with isotopically heavy Li-rich melt and later upon cooling the rim becomes low in $\delta^7\text{Li}$ due to diffusion-driven Li isotopic fractionation (e.g. Xiao et al. 2015). It is thus proposed that for the Gundeweyn samples, olivine best records the $\delta^7\text{Li}$ of the metasomatic

processes is different from that of the metasomatic processes responsible for LREE enrichment. Even though most of the earlier studies have underlined that Li isotopic disequilibria could not survive due to the very high diffusion rate of Li (e.g., Jeffcoate et al. 2007; Rudnick and Ionov 2007; Aulbach and Rudnick 2009; Halama et al. 2009), Vlastel'ic et al. (2009) argued that HIMU mantle has distinctly elevated $\delta^7\text{Li}$ and that Li isotopic heterogeneities could survive diffusion over 1–2 billion years in the mantle. Therefore, it is considered that the disequilibrium of Li isotopes in the mantle peridotites could be preserved for a long period (Tang et al. 2009). The heavy $\delta^7\text{Li}$ values (up to 6.2‰) in olivine from the HIMU lavas from the Cook-Austral volcanic chain reported by Chan et al. (2009). As a result, the HIMU-like Li isotopic compositions in some olivine (up to 6.3‰) grains indicate that Gundeweyn peridotites most probably experienced metasomatism by fluids/melts possibly derived from HIMU like asthenospheric Afar plume (Beccaluva et al. 2011), which is very near to the study area (Fig. 1). Some orthopyroxene and clinopyroxene also reveal heavy rim and light core Li isotopic compositions and some other pyroxene grains show the reverse. Overall, the three minerals phase does not show systematic regular $\delta^7\text{Li}$ zonation, indicating the presence of complex processes controlling the Li distribution in samples. The irregular variation of $\delta^7\text{Li}$ in core-rim of minerals grains from depleted and enriched Gundeweyn mantle xenoliths indicate recent diffusive fractionation of Li induced by percolation of metasomatic melt shortly before entrainment, transportation, eruption and cooling. This is consistent with observations reported by Xu et al. (2013).

Many recent studies have suggested that Li diffusion in clinopyroxene is faster than in olivine (Jeffcoate et al. 2007; Rudnick and Ionov 2007; Parkinson et al. 2007). If so, the low $\delta^7\text{Li}$ clinopyroxene relative to $\delta^7\text{Li}$ olivine in the Gundeweyn peridotites (Fig. 3d), coupled with the lack of correlations between $\delta^7\text{Li}$ clinopyroxene and other parameters (5e), may reflect recent diffusion of Li into clinopyroxene and associated kinetic isotope fractionation, possibly during transport in the basaltic host rock. Furthermore, diffusion-driven Li isotopic fractionation will produce lower $\delta^7\text{Li}$ in clinopyroxene than in coexisting olivines (Aulbach and Rudnick 2009; Ionov and Seitz 2008; Rudnick and Ionov 2007; Tang et al. 2007) because the diffusivity of Li is much higher in pyroxene (^6Li diffuses faster than ^7Li) than in olivine (Dohmen et al. 2010; Parkinson et al. 2007). There is no systematic correlation between $\delta^7\text{Li}$ olivine and LREE enrichment and Sr isotope in clinopyroxene (Fig. 5d,e), and oxygen isotope composition in olivine (Fig. 5f). This interpretation is also consistent with the lack of correlation between Li in olivine and $(\text{La}/\text{Yb})_N$ in clinopyroxene and modal abundances of the minerals indicating that diffusion-driven Li isotopic fractionation related to melt-peridotite interaction and incompatible enrichment events occur at different times. The clinopyroxene from Gundeweyn peridotites are fall within the range of the Tanzanian clinopyroxene peridotite in $\delta^7\text{Li}$. This could be related diffusion fractionation $\delta^7\text{Li}$ that can occur during peridotite-melt/fluid interaction before or coincide with the entrainment into host magmas and the transport of the mantle xenolith to the surface. Similar interpretations are also made from worldwide peridotite (e.g. Aulbach and Rudnick, 2009; Aulbach et al., 2008; Gallagher and Elliott, 2009; Halama et al., 2009; Ionov and Seitz, 2008; Rudnick and Ionov, 2007).

SUMMARY AND CONCLUSION

The development of Li elemental and isotope analysis has been used to trace several geological processes related to melt/fluid-rock reaction or metasomatism (Rudnick and Ionov, 2007; Ackerman et al., 2013; Gu et al., 2016), cooling processes upon eruption (Ionov and Seitz, 2008), and the interaction of the peridotite with the host magma during entrainment and ascent (Aulbach and Rudnick, 2009).

Olivines in the lherzolites and harzburgite from the present samples have generally homogeneous Li contents, higher than mantle olivine (1.6–1.9 ppm; Eggins et al. 1998; Seitz and Woodland 2000), and fall within the range of normal mantle olivine in $\delta^7\text{Li}$ (average +2.2 to 6.0‰ in lherzolites and average 3.5‰ in harzburgite), indicating isotopically heavy Li-rich asthenospheric melt addition to the lithospheric mantle beneath the area. Orthopyroxene and clinopyroxene show lower Li contents and isotopic composition than coexisting olivine. Most olivine grains display Li isotopic zonation with heavy cores and light rims while most pyroxene grains show increase in $\delta^7\text{Li}$ from core to rim. The observed systematic inter-mineral variations of Li concentrations and isotopic compositions could be combined effects of diffusion-induced fractionation of Li isotopes during melt/fluid-peridotite interactions and cooling, possibly during the transport in the basaltic host rock. Thus, the significant Li enrichment and large isotopic fractionation during melt/fluid-peridotite reactions imply that Li abundance and isotopes may be useful tracers of mantle metasomatic processes. Generally, the large variation in Li isotopic compositions within and between grains in samples reflect the effect of diffusion-driven isotopic fractionation during peridotite-melt interaction and cooling processes.

References

- Ackerman, L., Spaček, P., Magna, T., Ulrych, J., Svojtka, M., Hegner, E., Balogh, K. (2013) Alkaline and carbonate-rich melt metasomatism and melting of sub-continental lithospheric mantle: Evidence from mantle xenoliths, NE Bavaria, Bohemian Massif. *Jour. Petrol.*, v.54, pp.2597–2633
- Agostini, S., Ryan, J.G., Tonarini, S., Innocenti, F. (2008) Drying and drying of a subducted slab: coupled Li and B isotope variations in Western Anatolia Cenozoic Volcanism. *Earth Planet. Sci. Lett.*, v.272, pp.139–147
- Alemayehu, M., Zhang, H.F., Zhu, B., Fentie, B., Abraham, A., Haji, M. (2016a) Petrological constraints on evolution of continental lithospheric mantle beneath the northwestern Ethiopian plateau: Insight from mantle xenoliths from the Gundeweyn area, East Gojam, Ethiopia. *Lithos*, v.240–243, pp.295–308
- Alemayehu, M., Zhang, H.F., Sakyi, P.A. (2016b) Nature and evolution of lithospheric mantle beneath the southern Ethiopian rift zone: Evidence from petrology and geochemistry of mantle xenoliths. *Internat. Jour. Earth Sci.*, DOI: 10.1007/s00531-016-1342-z
- Alemayehu, M., Zhang, H. and Aulbach, S. (2016c) Evolution and persistence of fertile lithospheric mantle beneath the northwestern Ethiopian plateau: Evidence from petrography and chemical composition of mantle xenoliths from Gundeweyn. *Tectonophysics*, v. __, pp. __
- Alemayehu, M., Zhang, H.F., Aulbach, S. (2016d) Evaluation of mantle processes in an extensional regime: Evidence from *in-situ* O and Sr isotope systematics of mantle xenoliths from Ethiopia. *Jour. Geol.*, v.124, pp.603–616
- Anders, E., Grevesse, N. (1989) Abundances of the elements: meteoritic and solar. *Geochim. Cosmochim. Acta*, v.53, pp.197–214
- Aulbach, S., Rudnick, R.L. (2009) Origins of non-equilibrium lithium isotope fractionation in xenolithic peridotite minerals: examples from Tanzania. *Chem. Geol.*, v.258, pp.17–27
- Aulbach, S., Rudnick, R.L., McDonough, W.F. (2008) Li-Sr-Nd isotope signatures of the plume and cratonic lithospheric mantle beneath the margin of the rifted Tanzanian craton (Labait). *Contrib. Mineral. Petrol.*, v.155, pp.79–92
- Ayalew, D., Arndt, N., Bastien, F., Yirgu, G., Kieffer, B. (2009) A new mantle xenolith locality from Simien shield volcano, NW Ethiopia. *Geol. Magz.*, v.146, pp.144–149
- Ayalew, D., Yirgu, G., Ketefo, E., Barbey, P., Ludden, J. (2003) Intrusive equivalents of flood volcanics: Evidence from petrology of xenoliths in Quaternary Tana basanites Ethiopia. *Ethiopian Jour. Sci.*, v.26, pp.93–102
- Baker, B.H., Mohr, P., Williams, R.A.J. (1972) Geology of the Eastern Rift System of Africa. *Geology*, v.100, pp.200–211
- Baker, J., Thirlwall, M., Menzies, M. (1996) Sr-Nd-Pb isotopic and trace element evidence for crustal contamination of plume derived flood basalts; Oligocene flood volcanism in western Yemen. *Geochim. Cosmochim. Acta*, v.60, pp.2559–2581
- Beccaluva, L., Bianchini, G., Natali, C., Siena, F. (2009) Continental Flood Basalts and Mantle Plumes: a Case Study of the Northern Ethiopian Plateau. *Jour. Petrol.*, v.50, pp.1377–1403
- Beccaluva, L., Bianchini, G., Ellam, R.M., Natali, C., Santato, A., Siena, F., Stuart, F.M. (2011) Peridotite xenoliths from Ethiopia: inferences on mantle processes from plume to rift settings. *Geol. Soc. Am. Spec. Papers*, v.478, pp. 77–104
- Beck, P., Chaussidon, M., Barrat, J.A., Gillet, P., Bohn, M. (2006) Diffusion induced Li isotopic fractionation during the cooling of magmatic rocks: the case of pyroxene phenocrysts from nakhlite meteorites. *Geochim. Cosmochim. Acta*, v.70, pp.4813–4825
- Bedini, R.M., Bodinier, J.L. (1999) Distribution of incompatible trace elements between the constituents of spinel peridotite xenoliths: ICP-MS data from the East African Rift. *Geochim. Cosmochim. Acta*, v.63, pp.3883–3900
- Bedini, R.M., Bodinier, J.L., Dautria, J.M., Morten, L. (1997) Evolution of LILE enriched small melt fractions in the lithospheric mantle: a case study from the East African Rift. *Earth Planet. Sci. Lett.*, v.153, pp.67–83
- Bell, D.R., Hervig, R.L., Buseck, P.R. (2005) Li-isotope studies of olivine mantle xenoliths by SIMS. *Abstract, Lunar Planet. Sci.*, v. XXXVI, League City.
- Berckhemer, H., Bartelsen, H., Behle, A., Burkhardt, H., Gebrande, H., Makris, J., Menzel, H., Müller, H., Veis, R. (1975) Deep seismic soundings in the Afar region and on the high land of Ethiopia. *In: A. Pilger and A. Eoesler (Eds.), Afar Depression of Ethiopia*. Schweizerbart, Stuttgart, pp.89–107.
- Bianchini, G., Julia, G., Bryce, J.G., Blichert-Toft, J., Beccaluva, L., Natali, C. (2014) Mantle dynamics and secular variations beneath the East African Rift: Insights from peridotite xenoliths (Mega, Ethiopia). *Chem. Geol.*, v.386, pp.49–58.
- Bouman, C., Elliott, T., Vroon, P.Z. (2004) Lithium inputs to subduction zones. *Chem. Geol.*, v.212, pp.59–79.
- Brenan, J.M., Neroda, E., Lundstrom, C.C., Shaw, H.F., Ryerson, F.J., Phinney, D.L. (1998) Behaviour of boron, beryllium and lithium during melting and crystallization: constraints from mineral-melt partitioning experiments. *Geochim. Cosmochim. Acta*, v.62, pp.2129–2141.
- Brooker, R.A., James, R.H., Blundy, J.D. (2004) Trace elements and Li isotope systematics in Zabargad peridotites: evidence of ancient subduction processes in the Red Sea mantle. *Chem. Geol.*, v.212, pp.179–204.
- Caciagli, N., Brenan, J.M., McDonough, W.F., Phinney, D. (2011) Mineral-fluid partitioning of lithium and implications for slab-mantle interaction. *Chem. Geol.*, v.280, pp.384–398.
- Chan, L.H., Edmond, J.M. (1988) Variations of lithium isotope composition in the marine environment: a preliminary report. *Geochim. Cosmochim. Acta*, v.52, pp.1711–1717.
- Chan, L.H., Frey, F.A. (2003) Lithium isotope geochemistry of the Hawaiian plume: results from the Hawaii Scientific Drilling Project and Koolau volcano. *Geochim. Geophys. Geosyst.* doi:10.1029/2002GC000365
- Chan, L.H., Kastner, M. (2000) Lithium isotopic compositions of pore fluids and sediments in the Costa Rica subduction zone: implications for fluids processes and sediments contribution to the arc volcanoes. *Earth Planet. Sci. Lett.*, v.183, pp.275–290.
- Chan, L.H., Edmond, J.M., Thompson, G., Gillis, K. (1992) Lithium isotopic composition of submarine basalts—implications for the lithium cycle in the oceans. *Earth Planet. Sci. Lett.*, v.108, pp.151–160.
- Chan, L.H., Gieskes, J.M., You, C.F., Edmond, J.M. (1994) Lithium isotope geochemistry of sediments and hydrothermal fluids of the Guaymas Basin, Gulf of California. *Geochim. Cosmochim. Acta*, v.58, pp.4443–4454.
- Chan, L.H., Alt, J.C., Teagle, D.A.H. (2002a) Lithium and lithium isotope profiles through the upper oceanic crust: a study of seawater basalt exchange at ODP sites 504B and 896A. *Earth Planet. Sci. Lett.*, v.201, pp.187–201
- Chan, L.H., Leeman, W.P., You, C.F. (2002b) Lithium isotopic composition of Central American volcanic arc lavas: implications for modification of subarc mantle by slab-derived fluids: correction. *Chem. Geol.*, v.182, pp.293–300
- Chan, L.H., Lassiter, J.C., Hauri, E.H., Hart, S.R., Blusztajn, J. (2009) Lithium isotope systematics of lavas from the Cook-Austral Islands: constraints on the origin of HIMU mantle. *Earth Planet. Sci. Lett.*, v.277, pp.433–442.
- Coltorti, M., Bonadiman, C., Hinton, R.W., Siena, F., Upton, B.G.J. (1999)

- Carbonatite metasomatism of the oceanic upper mantle: evidence from clinopyroxenes and glasses in ultramafic xenoliths of Grande Comore, Indian Ocean. *Jour. Petrol.*, v.40, pp.133–165
- Coogan, L.A., Kasemann, S.A., Chakraborty, S. (2005) Rates of hydrothermal cooling of new oceanic upper crust derived from lithium-geospeedometry. *Earth Planet. Sci. Lett.*, v.240, pp.415–424
- Coogan, L.A. (2011) Preliminary experimental determination of the partitioning of lithium between plagioclase crystals of different anorthite contents. *Lithos*, v.125, pp.711–715
- Conticelli, S., Sintoni, M.F., Abebe, T., Mazzarini, F., Manetti, P. (1999) Petrology and geochemistry of ultramafic xenoliths and host lavas from Ethiopian volcanic province; an insight into the upper mantle under eastern Africa. *Acta Vulcanol.*, v.11, pp.143–151
- Courtillot, V., Davaille, A., Besse, J., Joann (2003) Three distinct types of hot spots in the Earth's mantle. *Earth Planet. Sci. Lett.*, v.205, pp.295–308
- Dawson, J.B. (1984) Contrasting types of upper mantle metasomatism? *In: Kornprobst, J. (Ed.), Kimberlites II. Elsevier Amster*, no.11, pp.519–548
- Decitre, S.E., Deloule, E., Reisberg, L., James, R., Agrinier, P., Me' vel, C. (2001) Behavior of Li and its isotopes during serpentinization of oceanic peridotites. *Geochem. Geophys. Geosyst.*, v.2, pp.178
- Dohmen, R., Kasemann, S.A., Coogan, L., Chakraborty, S. (2010) Diffusion of Li in olivine. Part I: Experimental observations and a multi species diffusion model. *Geochim. Cosmochim. Acta*, v.74, pp.274–292
- Ebinger, C., Bechtel, C., Forsyth, D., Bowin, C. (1989) Effective elastic plate thickness beneath the east African and Afar plateaus and dynamic compensation for the uplifts. *Jour. Geophys. Res.*, v.94, pp.2883–2901
- Ebinger, C.J., Yemane, T., Weldable, G., Agonising, J.L., Walter, R.C. (1993) Late Eocene-Recent volcanism and faulting in the southern main Ethiopian rift. *Jour. Geol. Soc. London*, v.50, pp.99–108
- Ebinger, C.J., Sleep, N.H. (1998) Cenozoic magmatism throughout East Africa resulting from impact of a single plume. *Nature*, v.395, pp.788–790
- Eggins, S.M., Rudnick, R.L., McDonough, W.F. (1998) The composition of peridotites and their minerals: a laser-ablation ICP-MS study. *Earth Planet. Sci. Lett.*, v.154, pp.53–71
- Ferrando, S., Frezzotti, M.L., Neumann, E.R., Astis, D.G., Peccerillo, A., Dereje, A., Gezahegn, Y., Teklewold, A. (2007) Composition and thermal structure of the lithosphere beneath the Ethiopian plateau: evidence from mantle xenoliths in basanites, Injibara, Lake Tana Province. *Mineral. Petrol.*, v.93, pp.47–78
- Flesh, G.D., Anderson, A.R., Svec, H.J. (1973) A secondary isotopic standard for $^7\text{Li}/^6\text{Li}$ determination. *Internat. Jour Mass Spectrom. Ion. Phys.*, v.12, pp.265–272
- Frezzotti, M.L., Ferrando, S., Peccerillo, A., Petrelli, M., Tecce, F., Perucchi, A. (2010) Chlorine-rich metasomatic $\text{H}_2\text{O}-\text{CO}_2$ fluids in amphibole-bearing peridotites from Injibara (Lake Tana region, Ethiopian plateau): Nature and evolution of volatiles in the mantle of a region of continental flood basalts. *Geochim. Cosmochim. Acta*, v.74, pp.3023–3039
- Furman, T., Graham, D. (1999) Erosion of lithospheric mantle beneath the East African Rift system: Geochemical evidence from the Kivu volcanic province. *Lithos*, v.48, pp.237–262
- Furman, T., Kaleta, K., Bryce, J., Hanan, B.B. (2006) Tertiary Mafic Lavas of Turkana, Kenya: Constraints on East African Plume Structure and the Occurrence of High-micro Volcanism in Africa. *Jour. Petrol.*, v.47, pp.1221–1244
- Gallagher, K., Elliott, T. (2009) Fractionation of lithium isotopes in magmatic systems as a natural consequence of cooling. *Earth Planet. Sci. Lett.*, v.278, pp.286–296
- Gao, S., Rudnick, R., Carlson, R.W., McDonough, W.F., Liu, Y.S. (2002) Re-Os evidence for replacement of ancient mantle lithosphere beneath the North China Craton. *Earth Planet. Sci. Lett.*, v.198, pp.307–322
- George, R., Rogers, N., Kelley, S. (1998) Earliest magmatism in Ethiopia: evidence for two mantle plumes in one flood basalt province. *Geology*, v.26, pp.923–926
- George, R., Rogers, N. (2002) Plume dynamics beneath the African plate inferred from the geochemistry of the Tertiary basalts of southern Ethiopia. *Contrib. Mineral. Petrol.*, v.144, pp.286–304
- Halama, R., Savov, I.P., Rudnick, R.L., McDonough, W.F. (2009) Insights into Li and Li isotope cycling and sub-arc metasomatism from veined mantle xenoliths, Kamchatka. *Contrib. Mineral. Petrol.*, v.158(2), pp.197–222
- Ionov, D.A., Seitz, H.M. (2008) Lithium abundances and isotopic compositions in mantle xenoliths from subduction and intra-plate settings: mantle sources vs. eruption histories. *Earth Planet. Sci. Lett.*, v.266, pp.316–331
- James, R.H., Rudnicki, M.D., Palmer, M.R. (1999) The alkali element and boron geochemistry of the Escanaba Trough sediment-hosted hydrothermal system. *Earth Planet. Sci. Lett.*, v.171, pp.157–169
- Jeffcoate, A.B., Elliott, T. (2003) Tracing recycled Li in the mantle: insights into mantle heterogeneities. *EOS Trans. AGU*, v.84, pp.V52A–0416
- Jeffcoate, A.B., Elliott, T., Kasemann, S.A., Ionov, D., Cooper, K., Brooker, R. (2007) Li isotope fractionation in peridotites and mafic melts. *Geochim. Cosmochim. Acta*, v.71, pp.202–218
- Kaesler, B., Olker, B., Kalt, A., Altherr, R., Pettko, T. (2009) Pyroxenite xenoliths from Marsabit (Northern Kenya): evidence for different magmatic events in the lithospheric mantle and interaction between peridotite and pyroxenite. *Contrib. Mineral. Petrol.*, v.157, pp.453–472
- Kampunzu, A.B., Mohr, P. (1991) Magmatic evolution and petrogenesis in the East African Rift System. *In: Kampunzu, A.B., Lubala, R.T. (eds) Magmatism in extensional structural settings. Springer, Berlin Heidelberg New York*, pp.85–136
- Kaliwoda, M., Ludwig, T., Altherr, R. (2008) A new SIMS study of Li, Be, B and $\delta^7\text{Li}$ in mantle xenoliths from Harrat Uwayrid (Saudi Arabia). *Lithos*, v.106(3–4), pp.261–279
- Kieffer, B., Arndt, N., Lapierre, H., Bastien, F., Bosch, D., Pecher, A., Yirgu, G., Ayalew, D., Weis, D., Jerram, D.A., Keller, F., Meugniot, C. (2004) Flood and shield basalts from Ethiopia: Magmas from the African superswell. *Jour. Petrol.*, v.45, pp.793–834
- Kobayashi, K., Tanaka, R., Moriguti, T., Shimizu, K., Nakamura, E. (2004) Lithium, boron and lead isotope systematics of glass inclusions in olivines from Hawaiian lavas: evidence for recycled components in the Hawaiian plume. *Chem. Geol.*, v.212, pp.143–161
- Kosiler, J., Magna, T., Mlcoch, B., Mixa, P., Ny't, D., Holub, F.V. (2009) Combined Sr, Nd, Pb and Li isotope geochemistry of alkaline lavas from northern James Ross Island (Antarctic Peninsula) and implications for back-arc magma formation. *Chem. Geol.*, v.258, pp.207–218
- Krienitz, M.S., Garbe-Schonberg, C.D., Romer, R.L., Meixner, A., Haase, K.M., Stronck, N.A. (2012) Lithium isotope variations in ocean island basalts: Implications for the development of mantle heterogeneity. *Jour. Petrol.*, v.53, pp.2333–2347
- Li, S.G., Xiao, Y.L., Liou, D.L., Chen, Y.Z., Ge, N.J., Zhang, Z.Q., Sun, S.S., Cong, B.L., Zhang, R.Y., Hart, S.R., Wang, S.S. (1993) Collision of the North China and Yangtze Blocks and formation of coesite bearing eclogites—timing and processes. *Chem. Geol.*, v.109, pp.89–111
- Lorand, J.P., Reisberg, L., Bedini, R.M., Horan, M.F., Brandon, A.D., Neal, C.R. (2003) Platinum-group elements and melt percolation processes in Sidamo spinel peridotite xenoliths, Ethiopia, East African Rift. *Chem. Geol.*, v.196, pp.57–75
- McDonough, W.F., Sun, S.S. (1995) The composition of the Earth. *Chem. Geol.*, v.120, pp.223–253
- McDonough, W.F., Frey, F.A. (1989) Rare-earth elements in upper mantle rocks. *Rev. Mineral. Geochem.*, v.21, pp.99–145
- Meshasha, D., Shinjo, R., Matsumura, R., Chekol, T. (2011) Metasomatized lithospheric mantle beneath Turkana depression in southern Ethiopia (the East Africa Rift): geochemical and Sr-Nd-Pb isotopic characteristics. *Contrib. Mineral. Petrol.*, v.162, pp.889–907
- Lundstrom, C.C., Chaussidon, M., Hsui, A.T., Kelemen, P., Zimmerman, M. (2005) Observations of Li isotopic variations in the Trinity Ophiolite: evidence for isotopic fractionation by diffusion during mantle melting. *Geochim. Cosmochim. Acta*, v.69, pp.735–751
- Magna, T., Wiechert, U., Halliday, A.N. (2006) New constraints on the lithium isotope compositions of the Moon and terrestrial planets. *Earth Planet. Sci. Lett.*, v.243(3–4), pp.336–353
- Mallmann, G., O'Neill, H., Klemme, S. (2009) Heterogeneous distribution of phosphorus in olivine from otherwise well-equilibrated spinel peridotite xenoliths and its implications for the mantle geochemistry of lithium. *Contrib. Mineral. Petrol.*, v.158, pp.485–504
- Marschall, H.R., Pogge von Strandmann, P.A.E., Seitz, H.M., Elliott, T., Niu, Y. (2007) The lithium isotopic composition of orogenic eclogites and deep subducted slabs. *Earth Planet. Sci. Lett.*, v.262, pp.563–580
- Menzies, M., Xu, Y.G., Zhang, H.F., Fan, W.M. (2007) Integration of geology, geophysics and geochemistry: a key to understanding the North China Craton. *Lithos*, v.96, pp.1–21
- Mercier, J.C.C., Nicolas, A. (1975) Textures and fabrics of upper mantle

- peridotites as illustrated by basalt xenoliths. *Jour. Petrol.*, v.16, pp.454–487
- Merla, G., Abbate, E., Azzaroli, A., Bruni, P., Canuti, P., Fazzuoli, M., Sagri M, Tacconi P (1973) A geological map of Ethiopia and Somalia (1973) 1:2,000,000 and comment with a map of major landforms. National Council of Research (CNR), Roma, Italy
- Moriguti, T., Nakamura, E. (1998a) Across-arc variation of Li isotopes in lavas and implications for crust/mantle recycling at subduction zones. *Earth Planet. Sci. Lett.*, v.163, pp.167–174
- Moriguti, T., Nakamura, E. (1998b) High-yield lithium separation and the precise isotopic analysis for natural rock and aqueous samples. *Chem. Geol.*, v.145, pp.91–104
- Mungall, J.E. (2002) Empirical models relating viscosity and tracer diffusion in magmatic silicate melts. *Geochim Cosmochim Acta*, v.66, pp.125–143
- Nakamura, E., Kushiro, I. (1998) Trace element diffusion in jadeite and diopside melts at high pressures and its geochemical implication. *Geochim. Cosmochim. Acta*, v.62, pp.3151–3160
- Nishio, Y., Nakai, S., Yamamoto, J., Sumino, H., Matsumoto, T., Prihod'ko, V.S., Arai, S. (2004) Lithium isotopic systematics of the mantle-derived ultramafic xenoliths: implications for EM1 origin. *Earth Planet. Sci. Lett.*, v.217, pp.245–261
- Nishio, Y., Nakai, S., Kogiso, T., Barszczus, H.G. (2005) Lithium, strontium, and neodymium isotopic compositions of oceanic island basalts in the Polynesian region: constraints on a Polynesian HIMU origin. *Geochem. Jour.*, v.39, pp.91–103
- Nyblade, A.A., Owens, T.J., Gurrola, H., Ritsema, J., Langston, C.A. (2000) Seismic evidence for a deep upper mantle thermal anomaly beneath east Africa. *Geology*, v.28, pp.599–602
- Ottolini, L., Laporte, D., Raffone, N., Devidal, J.L., Le, F.B. (2009) New experimental determination of Li and B partition coefficients during upper mantle partial melting. *Contrib. Mineral. Petrol.*, v.157, pp.313–325
- Orlando, A., Abebe, T., Manetti, P., Santo, A.P., Corti, G. (2006) Petrology of mantle xenoliths from Megado and Dillo, Kenya rift, Southern Ethiopia. *Ophiolite*, v.31, pp.71–87
- Parkinson, I.J., Hammond, S.J., James, R.H., Rogers, N.W. (2007) High temperature lithium isotope fractionation: insights from lithium isotope diffusion in magmatic systems. *Earth Planet. Sci. Lett.*, v.257, pp.609–621
- Pearson DG, Canil D, Shirey SB (2003) Mantle samples included in volcanic rocks: xenoliths and diamonds. *In: Carlson RW. (Ed.), Treatise on Geochemistry*, vol. 2. Elsevier Ltd., pp.171–275.
- Piccardo, G.B., Zanetti, A., Muntener, O. (2007) Melt/peridotite interaction in the Southern Lanzo peridotite: field, textural and geochemical evidence. *Lithos*, v.94, pp.181–209
- Rampone, E., Romairone, A., Hofmann, A.W. (2004) Contrasting bulk and mineral chemistry in depleted peridotites: evidence for reactive porous flow. *Earth Planet. Sci. Lett.*, v.218, pp.491–506
- Reisberg, L., Lorand, J.B., Bedini, R.M. (2004) Reliability of Os model ages in pervasively metasomatized continental lithosphere: a case study of Sidamo spinel peridotite xenoliths (East African Rift, Ethiopia). *Chem. Geol.*, v.208, pp.119–140
- Richter, F.M., Davis, A.M., Depaolo, D.J., Watson, E.B. (2003) Isotope fractionation by chemical diffusion between molten basalts and rhyolite. *Geochim. Cosmochim. Acta*, v.67, pp.3905–3923
- Rogers, S., Dautria, J.M., Coulon, C., Pik, R., Yirgu, G., Michard, A., Legros, P., Ayalew, D. (1999) An insight on the nature, composition and evolution of the lithospheric mantle beneath the north-western Ethiopian plateau; the ultrabasic xenoliths from the Tana Lake Province. *Acta Vulcanol.*, v.11, pp.161–168
- Rooney, O., Furman, T., Yirgu, G., Ayalew, D. (2005) Structure of Ethiopian lithosphere: xenoliths evidence in the main Ethiopian Rift. *Geochim. Cosmochim. Acta*, v.69, pp.3889–3910
- Rudnick, R.L., McDonough, W.L., Chappell, B.W. (1993) Carbonate metasomatism in the northern Tanzanian mantle: petrographic and geochemical characteristics. *Earth Planet. Sci. Lett.*, v.114, pp.463–475
- Rudnick, R.L., Ionov, D.A. (2007) Lithium elemental and isotopic disequilibrium in minerals from peridotite xenoliths from Far East Russia: product of recent melt/fluid-rock reaction. *Earth Planet. Sci. Lett.*, v.256, pp.278–293
- Ryan, J.G., Kyle, P.R. (2004) Lithium abundance and lithium isotope variations in mantle sources: insights from intraplate volcanic rocks from Ross Island and Marie Byrd Land (Antarctica) and other oceanic islands. *Chem. Geol.*, v.212, pp.125–142
- Scholz, F., Hensen, C., Reitz, A., Romer, R.L., Liebetrau, V., Meixner, A., Weise, S.M., Haecckel, M. (2009) Isotopic evidence ($^{87}\text{Sr}/^{86}\text{Sr}$, $\delta^7\text{Li}$) for alteration of the oceanic crust at deep-rooted mud volcanoes in the Gulf of Cadiz, NE Atlantic Ocean. *Geochim. Cosmochim. Acta*, v.73(18), pp.5444–5459
- Seitz, H.M., Woodland, A.B. (2000) The distribution of lithium in peridotitic and pyroxenitic mantle lithologies—an indicator of magmatic and metasomatic processes. *Chem. Geol.*, v.166, pp.47–64
- Seitz, H.M., Brey, G.P., Lahaye, Y., Durali, S., Weyer, S. (2004) Lithium isotopic signatures of peridotite xenoliths and isotopic fractionation at high temperature between olivine and pyroxenes. *Chem. Geol.*, v.212, pp.163–177
- Shinjo, R., Chekol, T., Meshesha, D., Tatsumi, Y., Itaya, T. (2010) Geochemistry and geochronology of the mafic lavas from the southeastern Ethiopian rift (the East African Rift System): assessment of models on magma sources, plume-lithosphere interaction and plume evolution. *Contrib. Mineral. Petrol.*, v.162, pp.209–230
- Spath, A., Le Roex, A.P., Opiyo-Akech, N. (2001) Plume-Lithosphere Interaction and the Origin of Continental Rift-related Alkaline Volcanism—the Chyulu Hills Volcanic Province, Southern Kenya. *Jour. Petrol.*, v.42(4), pp.765–787
- Stewart, K., Rogers, N. (1996) Mantle plume and lithosphere contributions to basalts from southern Ethiopia. *Earth Planet. Sci. Lett.*, v.139, pp.195–211
- Su, B.X., Zhang, H.F., Deloule, E., Sakyi, P.A., Xiao, Y., Tang, Y.J., Hu, Y., Ying, J.F., Liu, P.P. (2012) Extremely high Li and low $\delta^7\text{Li}$ signatures in the lithospheric mantle. *Chem. Geol.*, v.292–293, pp.149–157
- Su, B.X., Gu, X.Y., Deloule, E., Zhang, H.F., Li, Q.L., Li, X.H., Vigier, N., Tang, Y.J., Tang, G.Q., Liu, Y., Pang, K.N., Brewer, A., Mao, Q., Ma, Y.G. (2015) Potential Orthopyroxene, Clinopyroxene and Olivine Reference Materials for In Situ Lithium Isotope Determination. *Geostand. Geoanal. Res.*, v.39, pp.357–369
- Su, B.X., Zhang, H.F., Deloule, E., Vigier, N., Sakyi, P.A. (2014) Lithium elemental and isotopic variations in rock-melt interaction. *Chemie der Erde - Geochem.*, v.74(4), pp.705–713
- Tang, Y.J., Zhang, H.F., Ying, J.F. (2007a) Review of the lithium isotope systems as a geochemical tracer. *Internat. Geol. Rev.*, v.49, pp.274–388
- Tang, Y.J., Zhang, H.F., Nakamura, E., Moriguti, T., Kobayashi, K., Ying, J.F. (2007b) Lithium isotopic systematics of peridotite xenoliths from Hannuoba, North China Craton: implications for melt/rock interaction in the considerably thinned lithospheric mantle. *Geochim. Cosmochim. Acta.*, v.71, pp.4327–4341
- Tang, Y.J., Zhang, H.F., Deloule, E., Su, B.X., Ying, J.F., Xiao, Y., Hu, Y. (2012) Slab-derived lithium isotopic signatures in mantle xenoliths from northeastern North China Craton. *Lithos*, v.149, pp.79–90
- Tang, Y.J., Zhang, H.F., Nakamura, E., Moriguti, T., Kobayashi, K., Ying, J.F. (2007) Lithium isotopic systematics of peridotite xenoliths from Hannuoba, North China Craton: implications for melt/rock interaction in the considerably thinned lithospheric mantle. *Geochim. Cosmochim. Acta*, v.71, pp.4327–4341
- Tang, Y.J., Zhang, H.F., Nakamura, E., Ying, J.F. (2011) Multistage melt/fluid-peridotite interactions in the refertilized lithospheric mantle beneath the North China Craton: constraints from the Li–Sr–Nd isotopic disequilibrium between minerals of peridotite xenoliths. *Contrib. Mineral. Petrol.*, v.161, pp.845–861
- Teklay, M., Scherer, E.E., Mezger, K., Danyushevsky, L. (2010) Geochemical characteristics and Sr–Nd–Hf isotope compositions of mantle xenoliths and host basalts from Assab, Eritrea: implications for the composition and thermal structure of the lithosphere beneath the Afar Depression. *Contrib. Mineral. Petrol.*, v.159, pp.731–751
- Teng, F.Z., McDonough W.F., Rudnick R.L., Dalpe, C., Tomascak, P.B., Chappell, B.W., Gao, S. (2004) Lithium isotopic composition and concentration of the upper continental crust. *Geochim Cosmochim Acta* 68:4167–4178
- Teng FZ, McDonough WF, Rudnick RL, Walker RJ (2006) Diffusion driven extreme lithium isotopic fractionation in country rocks of the Tin Mountain pegmatite. *Earth Planet. Sci. Lett.*, v.243, pp.701–710

- Teng, F.Z., Rudnick, R.L., McDonough, W.F., Gao, S., Tomascak, P.B., Liu, Y.S. (2008) Lithium isotopic composition and concentration of the deep continental crust. *Chem. Geol.*, v.255, pp.47–59
- Tomascak, P.B. (2004) Developments in the understanding and application of lithium isotopes in the earth and planetary sciences. *In: Johnson, C.M., Beard, B.I., Albarede, F. (Eds.), Geochemistry of non-traditional stable isotope: reviews in mineralogy and geochemistry*, vol 55. Mineral Society of America, Washington DC, pp.153–195
- Tomascak, P.B., Tera, F., Helz, R., Walker, R.J. (1999) The absence of lithium isotope fractionation during basalt differentiation: new measurements by multicollector sector ICP-MS. *Geochim. Cosmochim. Acta*, v.63, pp.907–910
- Tomascak, P.B., Ryan, J.G., Defant, M.J. (2000) Lithium isotope evidence for light element decoupling in the Panama sub-arc mantle. *Geology*, v.28, pp.507–510
- Tomascak, P.B., Widom, E., Benton, L.D., Goldstein, S.L., Ryan, J.G. (2002) The control of lithium budgets in island arcs. *Earth Planet. Sci. Lett.*, v.196, pp.227–238
- Tomascak, P.B., Langmuir, C.H., le Roux, P.J., Shirey, S.B. (2008) Lithium isotopes in global mid-ocean ridge basalts. *Geochim. Cosmochim. Acta*, v.72, pp.1626–1637
- Tommasini, S., Manetti, P., Innocenti, I., Sintoni, M.F., Conticelli, S., Abebe, T. (2005) The Ethiopian sub-continental mantle domains: Geochemical evidence from Cenozoic massif lavas. *Mineral and Petrol.*, v.84, pp.259–281
- Toramaru, A., Fujii, N. (1986) Connectivity of melt phase in a partially molten peridotite. *Jour. Geophys. Res.*, v.91, pp.9239–9252.
- Van Orman, J.A., Grove, T.L., Shimizu, N. (2001) Rare earth element diffusion in diopside: influence of temperature, pressure, and ionic radius, and an elastic model for diffusion in silicates. *Contrib. Mineral. Petrol.*, v.141, pp.687–703
- Vlastelica, I., Koga, K., Chauvel, C., Jacques, G., Te'louk, P. (2009) Survival of lithium isotopic heterogeneities in the mantle supported by HIMU-lavas from Rurutu Island, Austral Chain. *Earth Planet. Sci. Lett.*, v.286, pp.456–466
- Von Bargen, N., Waff, H.S. (1986) Permeabilities, interfacial areas, and curvatures of partially molten systems: results of numerical computations of equilibrium microstructures. *Jour. Geophys. Res.*, v.91, pp.9261–9276.
- Wagner, C., Deloule, E. (2007) Behaviour of Li and its isotopes during metasomatism of French Massif Central lherzolites. *Geochim. Cosmochim. Acta*, v.71, pp.4279–4296
- Weeraratne, D.S., Forsythe, D.W., Fischer, K.M., Nyblade, A.A. (2003) Evidence for an upper mantle plume beneath the Tanzanian craton from Rayleigh wave tomography. *Jour. Geophys. Res.*, v.108, pp.2427
- Wolde, Gabriel, G., Aronson, J.L., Walter, R.C. (1990) Geology, geochronology and rift basin development in the central sector of the Main Ethiopia Rift. *Geol. Soc. Amer. Bull.*, v.102, pp.439–458
- Woodland, A.B., Seitz, H.M., Yaxley, G.M. (2004) Varying behaviour of Li in metasomatised spinel peridotite xenoliths from western Victoria, Australia. *Lithos*, v.75, pp.55–66.
- Wu, F.Y., Walker, R.J., Yang, Y.H., Yuan, H.L., Yang, J.H. (2006) The chemical-temporal evolution of lithospheric mantle underlying the North China Craton. *Geochim. Cosmochim. Acta*, v.70, pp.5013–5034
- Wunder, B., Meixner, A., Romer, R.L., Heinrich, W. (2006) Temperature dependent isotopic fractionation of lithium between clinopyroxene and high-pressure hydrous fluids. *Contrib. Mineral. Petrol.*, v.151, pp.112–120
- Xu, Y.G., Ma, J.L., Huang, X.L., Iizuka, Y., Chung, S.L., Wan, Y.B., Wu, X.Y. (2004) Early Cretaceous gabbroic complex from Yinan, Shandong Province: petrogenesis and mantle domains beneath the North China Craton. *Internat. Jour. Earth Sci.*, v.93, pp.1025–1041
- Yakob, J.L., Feineman, M.D., Deane, Jr. J.A., Egger, D.H., Penniston-Dorland, S.C. (2012) Lithium partitioning between olivine and diopside at upper mantle conditions: an experimental study. *Earth Planet. Sci. Lett.*, v.329–330, pp.11–21
- Yaxley, G.M., Crawford, A.J., Green, D.H. (1991) Evidence for carbonatite metasomatism in spinel peridotite xenoliths from western Victoria, Australia. *Earth Planet. Sci. Lett.*, v.107(2), pp.305–317
- Yemane, T., Wolde Gebriel, G., Tesfaye, S., Berhe, S.M., Durary, S., Ebinger, C.J., Kelley, S. (1999) Temporal and geochemical characteristics of Tertiary Volcanic Rocks and tectonic history in the southern main Ethiopia Rift and the adjacent volcanic fields. *Acta Vulcanol.* v.11, pp.99–119
- You, C.F., Chan, L.H. (1996) Precise determination of lithium isotopic composition in low concentration natural samples. *Geochim. Cosmochim. Acta*, v.60, pp.909–915.
- Zack, T., Tomascak, P.B., Rudnick, R.L., Dalpe, C., McDonough, W.F. (2003) Extremely light Li in orogenic eclogites: the role of isotope fractionation during dehydration in subducted oceanic crust. *Earth Planet. Sci. Lett.*, v.208, pp.279–290.
- Zanettine, B., Justin-Visentin, E., Nicoletti, M., Petrucciani, C. (1978) The evolution of the Chench escarpment and the Ganjuli graben (lake Abaya) in the southern Ethiopian rift. *Neu. Jah. Fur Geol. Palaent., Monatsh*, no.8, pp.473–490
- Zhang, L., Chan, L.H., Gieskes, J.M. (1998) Lithium isotope geochemistry of pore waters, Ocean Drilling Program Sites 918 and 919, Irminger Basin. *Geochim. Cosmochim. Acta*, v.62, pp.2437–2450
- Zhang, H.F., Goldstein, S.L., Zhou, X.H., Sun, M., Zheng, J.P., Cai, Y. (2008) Evolution of subcontinental lithospheric mantle beneath eastern China: Re-Os isotopic evidence from mantle xenoliths in Paleozoic kimberlites and Mesozoic basalts. *Contrib. Mineral. Petrol.*, v.155, pp.271–293
- Zhang, H.F., Deloule, E., Tang, Y.J., Ying, J.F. (2010) Melt/rock interaction in remains of re-fertilized Archean lithospheric mantle in Jiaodong Peninsula, North China Craton: Li isotopic evidence. *Contrib. Mineral. Petrol.*, v.160, pp.261–277.

(Received: 1 November 2016; Revised form accepted: 26 April 2017)